Malaysian Journal of Chemistry, 2021, Vol. 23(2), 63-73
(Special Issue: *IKM Pahang Branch Online Symposium 2021 – Chemistry for Sustainable World*)

Molecular Docking Analysis of Designed Ligands on VP40 of Ebola Virus

Nur Fadhilah Rahim[1], Mohamad Ariff Mohamad Yussoff[2], Khairul Bariyyah binti Abd Halim[2,3], Azzmer Azzar Abdul Hamid[2,3] and Shafida Abd Hamid[1*]

[1]Department of Chemistry, Kulliyyah of Science, International Islamic University Malaysia, 25200 Kuantan, Pahang

[2]Department of Biotechnology, Kulliyyah of Science, International Islamic University Malaysia, 25200 Kuantan, Pahang

[3]Research Unit for Bioinformatics and Computational Biology, Kulliyyah of Science, International Islamic University Malaysia, 25200 Kuantan, Pahang

*Corresponding author (e-mail: shafida@iium.edu.my)

Ebola virus consists of different structural proteins, each of which plays its roles in different aspects of the viral life cycle. Among them, VP40 plays a number of critical roles in the viral lifecycle such as regulating viral transcription and coordinating virion assembly and budding from infected cells. Due to the fact that VP40 plays a vital role in the Ebola virus life cycle, it is considered as a promising target for the treatment of Ebola virus infection. This study aims to design ligands that have the potential to inhibit the VP40-RNA binding site. A total of seventeen ligands were designed based on the modification Q-88 (ZINC ID: 1342431) scaffold. Q-88 gave the best binding free energy of -97.27 kJ/mol and docking score of -7.1 kcal/mol according to previous literature. The seventeen ligands were then simulated against the RNA binding site using AutoDock Vina. The results showed that all ligands hold high binding affinities with VP40 ranging from -5.5 kcal/mol to -6.9 kcal/mol. Additionally, Q-88 was redocked as reference to determine if the modified ligands can surpass the binding affinity of Q-88 under the same circumstance. This study revealed that the modification of chlorine atoms on the benzene group did not give much effect towards increasing the binding affinity of the complex. Therefore, it is suggested that further chemical modifications should be carried out based on the Q-88 scaffold without altering the chlorine atom in the benzene group of the compound.

Key words: Ebola virus, molecular docking, VP40, Q-88, Q-96

Received: November 2020; Accepted: January 2021

Viruses are small obligate intracellular parasites which contain either a RNA or DNA genome surrounded by a protective, virus-coded protein coat [1]. Viruses cannot reproduce by themselves, but once it infects a susceptible cell, they can direct the cell machinery to produce more viruses. A fully assembled infectious virus is called a virion and depending on the virus type, the nucleic acid can be single-stranded or double-stranded, linear or circular, and monopartite or segmented [2]. Ebola virus is one of the major causes of sickness and death around the world with the last epidemic occurring in West Africa particularly in Liberia, Sierra Leone and Guinea from 2014 – 2016.

Ebola virus (EBOV) is a hostile pathogen that belongs to the family of *Filoviridae* and is responsible for the highly fatal haemorrhagic fever syndrome in humans which is often termed as Ebola virus disease (EVD). Currently, there are five species of the genus Ebola virus identified, which include *Zaire ebolavirus* (EBOV – previously known as ZEBOV), *Sudan ebolavirus* (SUDV), *Tai Forest ebolavirus* (TAFV), *Bundibugyo ebolavirus* (BDBV) and *Reston ebolavirus* (RESTV) [3]. The first four viruses are known to infect humans which lead to severe haemorrhagic fever, while Reston virus is known to cause disease in non-human primates only and does not infect humans [4]. The virus targets the immune system of the body which causes harmful inflammatory responses such as a cytokine storm. This can lead to apoptosis of many cell types including vascular endothelium and lymphocytes, and in fatal cases terminates in multiple organ failure [5].

EBOV consists of different structural proteins, each of which plays its roles in different aspects of the viral life cycle. The seven structural proteins that could be targeted as potential inhibitors of the virus include glycoprotein (GP), nucleoprotein (NP), transcription activator (VP30), polymerase cofactor (VP35), matrix proteins VP24, VP40 and RNA polymerase (L) [6]. Among these EBOV proteins, the matrix protein, VP40 plays a number of critical roles in the viral lifecycle where it is

†Paper presented at the IKM Pahang Branch Online Symposium 2021 – Chemistry for Sustainable World

abundantly expressed during infection. Apart from regulating the viral transcription, VP40 coordinates virion assembly and budding from infected cells [7]. Due to the fact that VP40 plays a vital role in the EBOV life cycle, it is considered as a potential target for the treatment of its infection.

VP40 is a peripheral protein made up of 326 amino acids which localises under the lipid envelope of the virus where it bridges the viral lipid envelope and nucleocapsid [8]. VP40 is known to play a very important role in virus assembly and budding. A study by Noda *et al.* suggested that the Ebola virus VP40 has structural information necessary and sufficient to induce the formation of filamentous particles which then bud from the plasma membrane [9]. There is still no vaccine or specific medicine commercially available for the treatment of EVD [10]. Therefore, there is an urgent need for identification of effective therapy for controlling and preventing people from getting infected by this disease.

In silico approach is a useful method for discovering new lead drug candidates against the virus [11]. In a recent study, Traditional Chinese Medicine (TCM), Asinex and ZINC databases were used in a virtual screening to find and design inhibitor lead compounds drugs for VP40 [12]. Molecular modelling and computational chemistry based-computer aided drug design provide great help for efficient identification and optimisation of lead compounds [13]. Software programmes such as AutoDock and AutoDock Vina are widely used to search for potential inhibitors for protein targets. Computational method involves protein structure docked with individual drug molecule. Based on the binding affinity scores obtained, the best drug lead can be identified. Recently, we simulated 42 compounds against the RNA binding site and the top ten ligands were used as templates for similarity search in ZINC database, followed by structural-based virtual screening. Our results showed that Q-96 (ZINC ID: 1338855) is the best docked compound with a binding free energy of -7.5 kcal/mol [14]. Meanwhile, compound Q-88 (ZINC ID:1342431) having a chlorine substituent instead of a methyl group gave a comparable binding free energy of -7.1 kcal/mol (Figure 1).

We were interested to investigate the effect of a Cl substituent on the free binding energy of the analogues as its property is different from the methyl group property in Q-96. In the current work, we designed molecules based on compound Q-88 by modifying the position of chlorine atom on the benzene ring of the compound. Molecular docking was performed to screen the potential ligands as VP40 inhibitors. The types of interaction between the designed ligands and VP40 residues were also studied.

EXPERIMENTAL SECTION

1. Protein Structure

The crystal structure of the Ebola virus matrix protein VP40 in complex with RNA at 1.6 Å resolution was obtained from RCSB Protein Data Bank (PDB) with the corresponding PDB code of 1H2C. The three-dimensional structure of the target protein was cleaned by removing all water molecules and RNA in the complex in the pdb file format. The structure was visualised using PyMOL version 1.7.2.1. The RNA binding site for docking simulation was predicted using COACH.

2. Ligand Modification

The structures of the ligands were drawn using Chemsketch. All the ligands were designed by modifications based on ligand Q-88 (ZINC ID: 1342431) as this scaffold has shown good binding energy with VP40 based on our initial study [14]. Seventeen structures were modified by varying the position of the chlorine atom on the outer phenyl group. The smile notations acquired from Chemsketch were submitted to the Automated Topology Builder (ATB) to obtain the optimised 3D structures of the ligands. The files were then converted into pdb file to be used as input for the molecular docking.

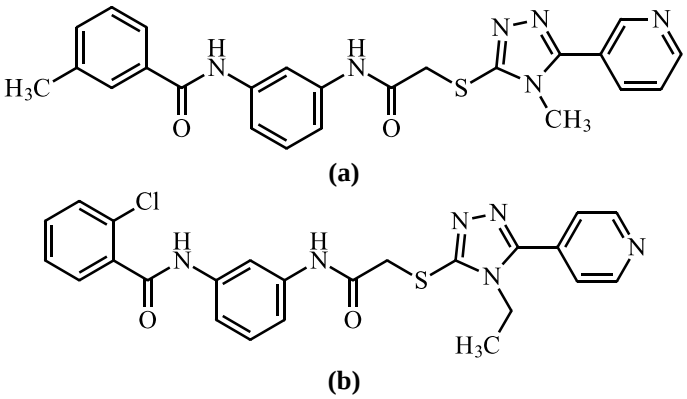

Figure 1. Structure of (a) Q-96 and (b) Q-88

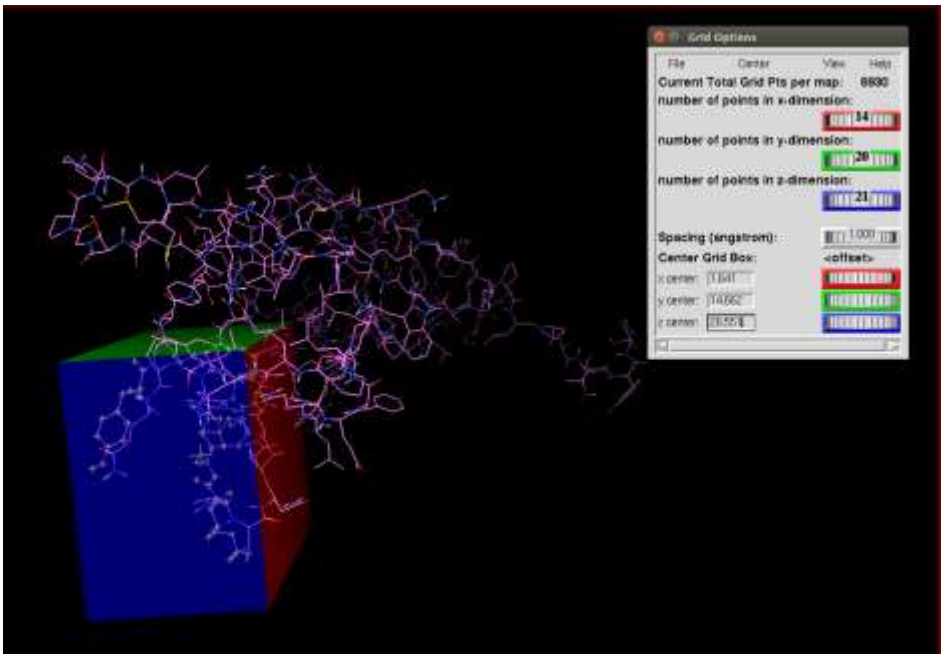

Figure 2. Grid box size containing RNA-interacting residue

3. Preparation of Protein and Ligand

The PDB files of the protein and ligand were prepared by using AutoDock tools before performing the molecular docking. AutoDock tools were used for addition of charges, polar hydrogens and the adjustment of other parameters. Hydrogen atoms were added to both protein and ligands as necessary in the system. Meanwhile, the non-polar hydrogens were merged together with the structure. Next, Kollman charges were added and Gasteiger charges were computed to the protein and ligands in order to incorporate partial charges and to calibrate scoring function.

AutoGrid 4.0 was used to generate grid maps and spacing. The grid was constructed with dimensions necessary to contain the RNA-interacting residues of Thr123, Phe125, Gly126, Lys127, Arg134 and Tyr171. The grid centre was set at 1.641, 14.662 and 28.551 for the x, y and z value respectively, with the size of the grid box set at 14.25 × 20.25 × 21 with a spacing of 1 Å. Figure 2 illustrated the grid box size which includes all the RNA-interacting residues involved in the binding activity.

4. Molecular Docking

AutoDock Vina version 1.1.2 software was employed to perform the molecular docking simulations [15]. All seventeen ligands were docked at the predicted RNA binding site. The compounds were ranked from the lowest to the highest according to the order of binding affinity. The docking outputs were analysed using AutoDockTools (ADT) while the ligand-protein interactions were visualised using PyMOL. Subsequently, LIGPLOT was performed to observe the hydrophobic interactions in the complex structures [16].

RESULTS AND DISCUSSION

1. Minimisation of Protein

Minimisation of energy of the target protein VP40 needs to be done prior to docking. The energy minimisation will provide a low energy conformation with suitable bond length and angles for better docking results [17]. Most structures downloaded in pdb files from the Protein Data Bank (PDB) contain no hydrogen atoms, thus they need to be added using ADT. Minimisation of protein was done by adding polar hydrogen atoms and removing water molecules for better binding activity with corresponding ligands. Kollman and Gasteiger charges were also computed to the protein to incorporate partial charges and to calibrate scoring function [18].

2. Modification of Ligands

Seventeen ligands based on the Q-88 (ZINC ID: 1342431) scaffold were modified as it had shown a good binding energy with VP40 [14]. Q-88 was obtained from ligand-based virtual screening that used ASN05439185 as a template with a similar scaffold. Tamilvanan and Hopper reported that ASN05439185 occupied the RNA binding region of VP40 with a Glide score of -7.39 and Glide energy of -44.72 kcal/mol [19]. The study also found two hydrogen bond interactions with amino acid residues Gly126 and Gln170 and four hydrophobic interactions with the amino acid residues Phe125, Ala128, Leu132 and Phe172. However, docking study by Mohamad Yussoff *et al*. using AutoDock Vina found that

ASN05439185 showed binding energy of -6.7 kcal/mol and formed three hydrogen bonds with residues Thr123, His124 and Gly126. Q-88 served as a better ligand that inhibits VP40 with binding energy of -7.1 kcal/mol compared to ASN05439185 and thus Q-88 was chosen to be modified and optimised [14].

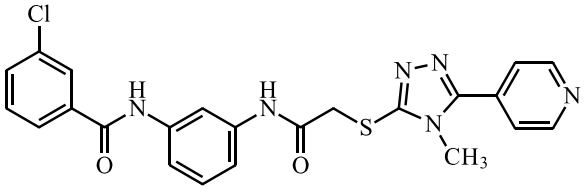

ASN05439185

Docking study by Mohamad Yussoff *et al*. also showed that the presence of methoxy (-OCH_3) substituent on the benzamide moiety decrease the energy value, while the presence of fluorine atom slightly decrease the binding energy. Q-88 and ASN05439185 have similar structures except for the types of alkyl group attached to the triazole ring and position of chlorine atom on the benzamide ring.

In this work, we vary the number and position of the chlorine atom on the benzamide moiety to investigate whether the chlorine atom plays an important role in binding of the ligands with the matrix protein VP40. The seventeen modified ligands are shown in Figure 3.

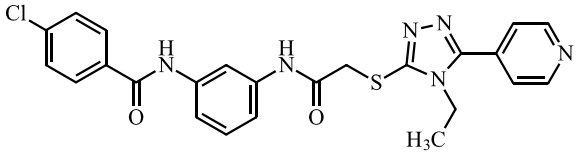

M-1

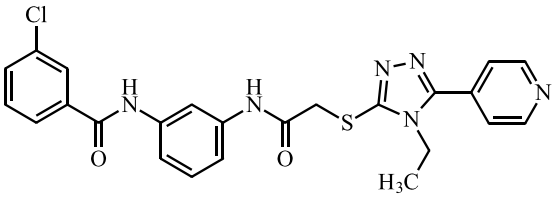

M-2

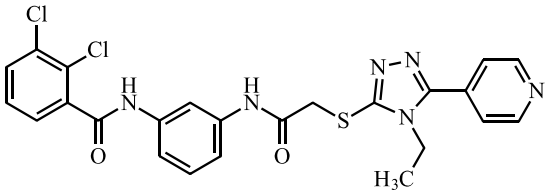

M-3

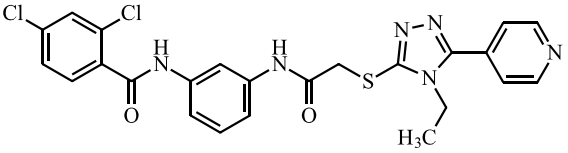

M-4

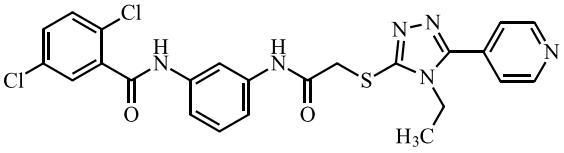

M-5

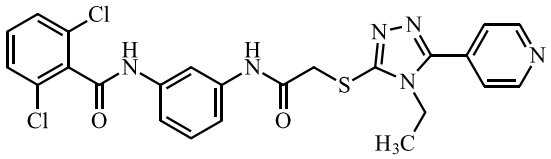

M-6

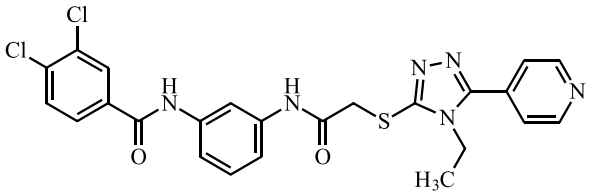

M-7

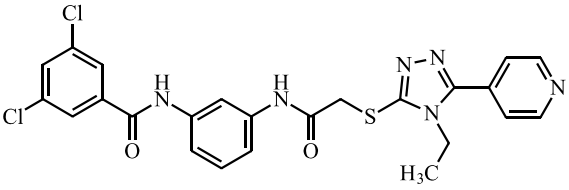

M-8

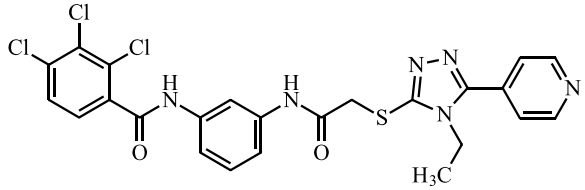

M-9

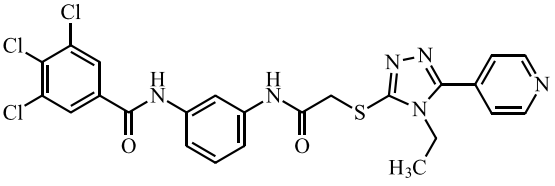

M-10

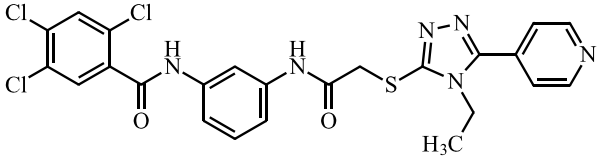

M-11

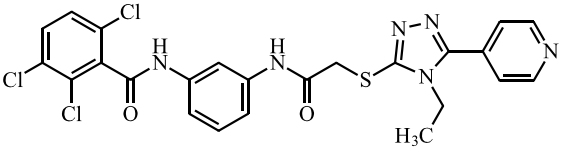

M-12

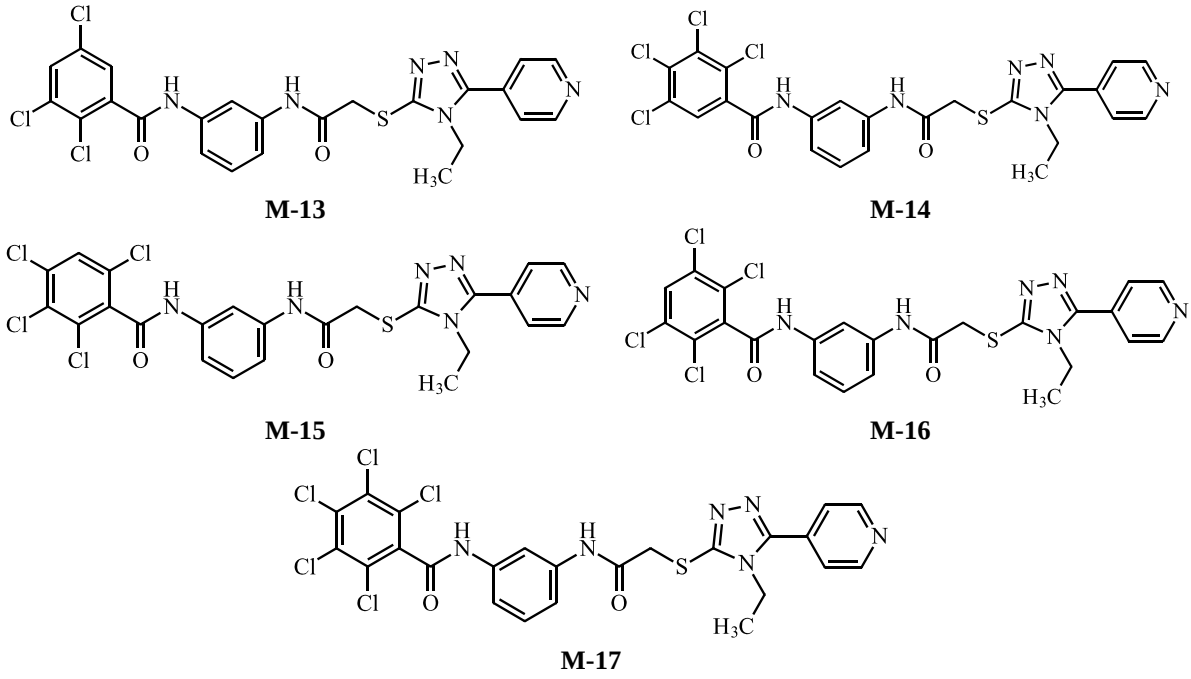

M-13 **M-14**

M-15 **M-16**

M-17

Figure 3. Modification of various ligands based on Q-88 scaffold

3. Molecular Docking

3.1. Binding Affinity and Hydrogen Bonds

The protein VP40 was docked with the seventeen ligands using AutoDock Vina version 1.1.2. AutoDock Vina was used as it provided faster calculation for binding affinity and also significantly improve the accuracy of the binding mode predictions [20]. The docking generated ten orientation values or modes for each of the ligands. The first conformation was considered as the best binding residue, thus the value of the first mode was noted.

Table 1 shows the binding affinity of all seventeen ligands starting from the lowest to the highest energy as well as residues involved in the binding interactions. The important residues in RNA binding activity for each compound are marked in bold. Q-88 was redocked as reference to determine if a ligand can surpass the binding affinity of Q-88 under the same circumstance. Overall, all ligands showed high binding affinities with VP40 ranging from -5.5 kcal/mol to -6.9 kcal/mol.

Table 1. Docking results of seventeen ligands with matrix protein VP40

Ligands	Binding affinity (kcal/mol)	No of H-bonds	H-bond residues	Interacting residues
Q-88	− 7.1	2	Thr123, Gly126	Thr123, His124, **Phe125**, Gly126, Ala128, **Arg134**, Asn136, Gln170, Tyr171
M-1	− 6.9	4	His124, Gly126 (2), Gln170	Thr123, His 124, Gly126, Ala128, **Arg134**, Asn136, Gln170
M-16	− 6.9	-	-	His124, **Phe125**, Gly126, Ala128, Pro131, Gln170, Tyr171, Phe172, Thr173
M-11	− 6.8	-	-	Thr123, His124, Gly126, Ala128, Pro131, **Arg134**, Gln170, Tyr171

M-6	− 6.7	-	-	Thr123, His124, **Phe125**, Gly126, Ala128, Pro131, **Arg134**, Gln170, Tyr171
M-12	− 6.7	-	-	Thr123, His124, **Phe125**, Gly126, Ala128, Pro131, **Arg134**, Gln170, Tyr171
M-2	− 6.6	-	-	Thr123, His124, **Phe125**, Gly126, Ala128, **Arg134**, Gln170, Tyr171
M-8	− 6.6	-	-	Thr123, His124, **Phe125**, Gly126, Ala128, **Arg134**, Gln170, Tyr171
M-7	− 6.5	-	-	Thr123, His124, **Phe125**, Gly126, Ala128, Pro131, Gln170, Tyr171
M-3	− 6.4	3	His124, Gly126, Thr173	Thr123, His124, **Phe125**, Gly126, Lys127, Ala128, Gln170, Thr173
M-5	− 6.1	1	Gly126	Thr123, His124, **Phe125**, Gly126, Lys127, Ala128, **Arg134**, Gln170, Tyr171
M-9	− 6.0	2	Thr123, Gly126	Thr123, His124, **Phe125**, Gly126, Lys127, Ala128, **Arg134**, Gln170, Tyr171
M-10	− 6.0	3	Thr123, His124, Gly126	Thr123, His124, **Phe125**, Gly126, Lys127, Ala128, **Arg134**, Gln170, Tyr171
M-4	− 5.9	3	Thr123, His124, Gly126	Thr123, His124, Phe125, Gly126, Ala128, **Arg134**, Gln170, Tyr171
M-13	− 5.9	2	His124, **Arg134**	Thr123, His124, **Phe125**, Gly126, **Arg134**, Tyr171, Thr173
M-17	− 5.6	-	-	Thr123, His124, **Phe125**, Gly126, **Arg134**, Asn136, Tyr171, Thr173
M-14	− 5.5	-	-	His124, **Phe125**, Gly126, **Arg134**, Asn136, Thr173
M-15	− 5.5	-	-	His124, **Phe125**, Gly126, **Arg134**, Asn136,Tyr171, Thr173

Note: The bolded residues indicate the important residues in binding activity.

All the ligands showed close contact with Phe125 and/or Arg134 which were the two important residues in hindering binding with viral RNA [21]. Ligand M-1 and M-16 gave the best binding affinity of -6.9 kcal/mol. M-1 formed four hydrogen bonds with residues His124, Gly126 (2) and Gln170, compared to two hydrogen bonds with Q-88, while M-16 did not form any hydrogen bond. The existence of hydrogen bond between the ligand and matrix protein VP40 is important because the bond provides stability of the ligand into its binding position [15]. Interestingly, it was observed that the position of chlorine atom on ligand M-1 reduces the steric hindrance thus forming hydrogen bonds with the nearby O and N atoms as compared to the redocked Q-88 where no hydrogen bond was formed nearby the benzene ring.

Other than that, ligands M-3, M-4, M-5, M-9, M-10 and M-13 were involved in at least one or up to 3 hydrogen bonds with the protein, while, Thr123, His124 and Gly126 showed active participation in hydrogen bonding with a majority of the ligands. The binding sites involved in hydrogen bonding correlate with a study conducted by Mirza and Ikram [22] whereby hydrogen bond analysis showed that the O atoms actively participated in H-bonds with Thr123 and Thr173 while N atoms H-bond with His124. The binding complexes of these ligands with the protein were visualised in PyMOL and the top three visualised ligands are shown in Figure 4.

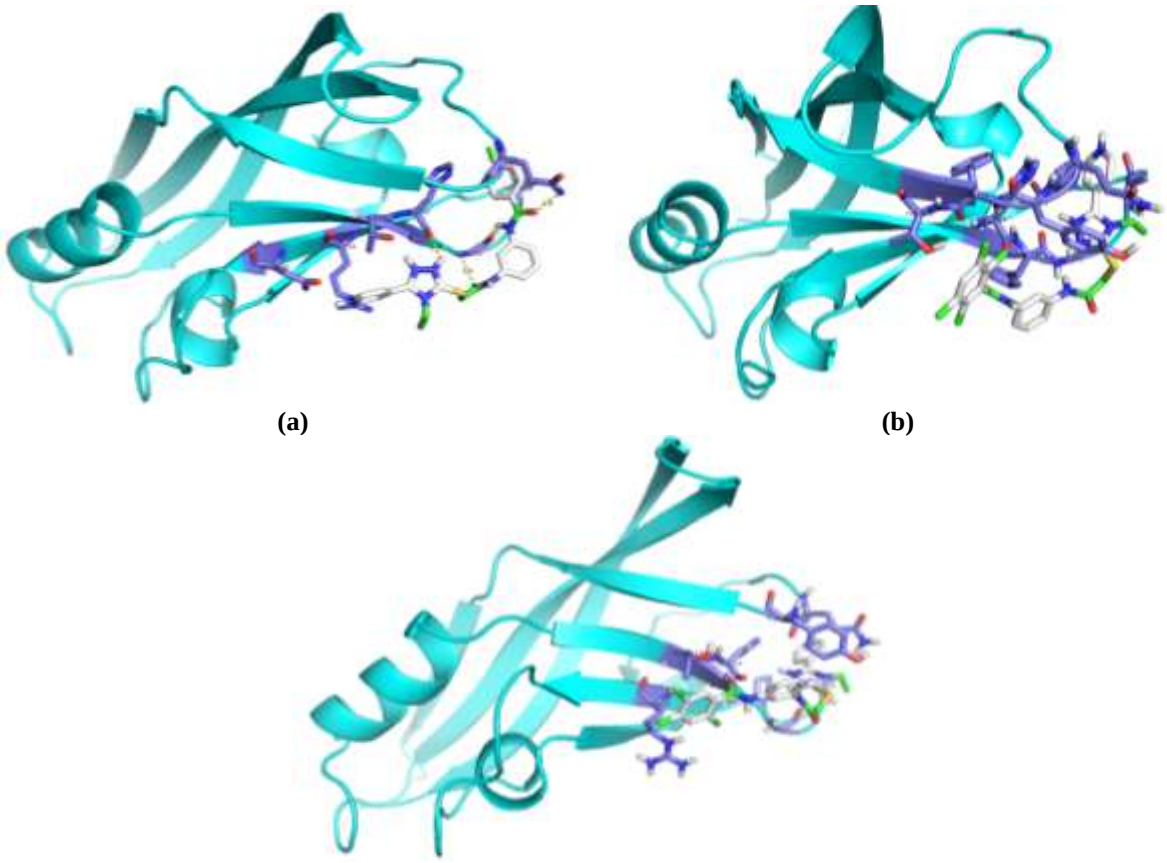

Figure 4. **(a)** Ligand M-1 complexed with VP40 (**b)** Ligand M-16 complexed with VP40 (**c)** Ligand M-11 complexed with VP40. The protein backbone is represented as a cartoon. The ligand (carbon in white) and active site residues (carbon in purple) are shown in stick representation.

Table 2. Hydrophobic interactions presented in protein complexes VP40

Ligands	No. of residue	Hydrophobic interaction residues
Q-88	11	Thr123, His124, Phe125, Gly126, **Lys127**, Ala128, **Pro131**, Arg134, Asn136, Gln170, Tyr171
M-1	10	Thr123, His 124, **Phe125,** Gly126, Ala128, **Pro131**, Arg134, Asn136, Gln170, **Tyr171**
M-16	10	**Thr123**, His124, Phe125, Gly126, Ala128, Pro131, Gln170, Tyr171, Phe172, Thr173
M-11	10	Thr123, His124, **Phe125**, Gly126, Ala128, Pro131, Arg134, **Asn136**, Gln170, Tyr171
M-6	10	Thr123, His124, Phe125, Gly126, Ala128, Pro131, Arg134, **Asn136**, Gln170, Tyr171
M-12	10	Thr123, His124, Phe125, Gly126, Ala128, Pro131, Arg134, **Asn136**, Gln170, Tyr171

M-2	8	Thr123, His124, Phe125, Gly126, Ala128, Arg134, Gln170, Tyr171
M-8	8	Thr123, His124, Phe125, Gly126, Ala128, Arg134, Gln170, Tyr171
M-7	9	Thr123, His124, Phe125, Gly126, Ala128, Pro131, Gln170, Tyr171, **Thr173**
M-3	11	Thr123, His124, Phe125, Gly126, Lys127, Ala128, **Arg134**, **Asn136**, Gln170, **Tyr171**, Thr173
M-5	8	Thr123, His124, Phe125, Gly126, Lys127, Ala128, Arg134, Tyr171
M-9	9	Thr123, His124, Phe125, Gly126, Lys127, Ala128, Arg134, Gln170, Tyr171
M-10	9	Thr123, His124, Phe125, Gly126, Lys127, Ala128, Arg134, Gln170, Tyr171
M-4	8	Thr123, His124, Phe125, Gly126, Ala128, Arg134, Gln170, Tyr171
M-13	8	Thr123, His124, Phe125, Gly126, Arg134, **Asn136**, Tyr171, Thr173
M-17	9	Thr123, His124, Phe125, Gly126, Arg134, Asn136, Tyr171, **Phe172**, Thr173
M-14	8	Thr123, His124, Phe125, Gly126, Arg134, Asn136, **Phe172**, Thr173
M-15	9	**Thr123**, His124, Phe125, Gly126, Arg134, Asn136,Tyr171, **Phe172**, Thr173

Note: The bolded residues indicate the important residues in binding activity.

3.2. Hydrophobic Interactions

Ligplot analysis was used to analyse the hydrophobic interaction of protein complexes. Hydrophobic interaction is important to be observed as it involves the increasing binding affinity between the target and ligand interfaces. The binding affinity associated with hydrophobic interactions can be optimised by incorporating them at the site of the hydrogen bonding [23].

Apart from hydrogen bonds, a large number of hydrophobic interactions were present with the residues surrounding RNA interacting site of VP40, as represented in Figure 5 for the top three ligands. Overall, Thr123, His124, Phe125, Gly126, Lys127, Ala128, Pro131, Arg134, Asn136, Gln170, Tyr171, Phe172 and Thr173 residues could form a network of hydrophobic interactions between the protein complexes. The hydrophobic interactions presented in protein complexes for each ligand are shown in Table 2, where the residues in bold were not present in the previous docking analysis.

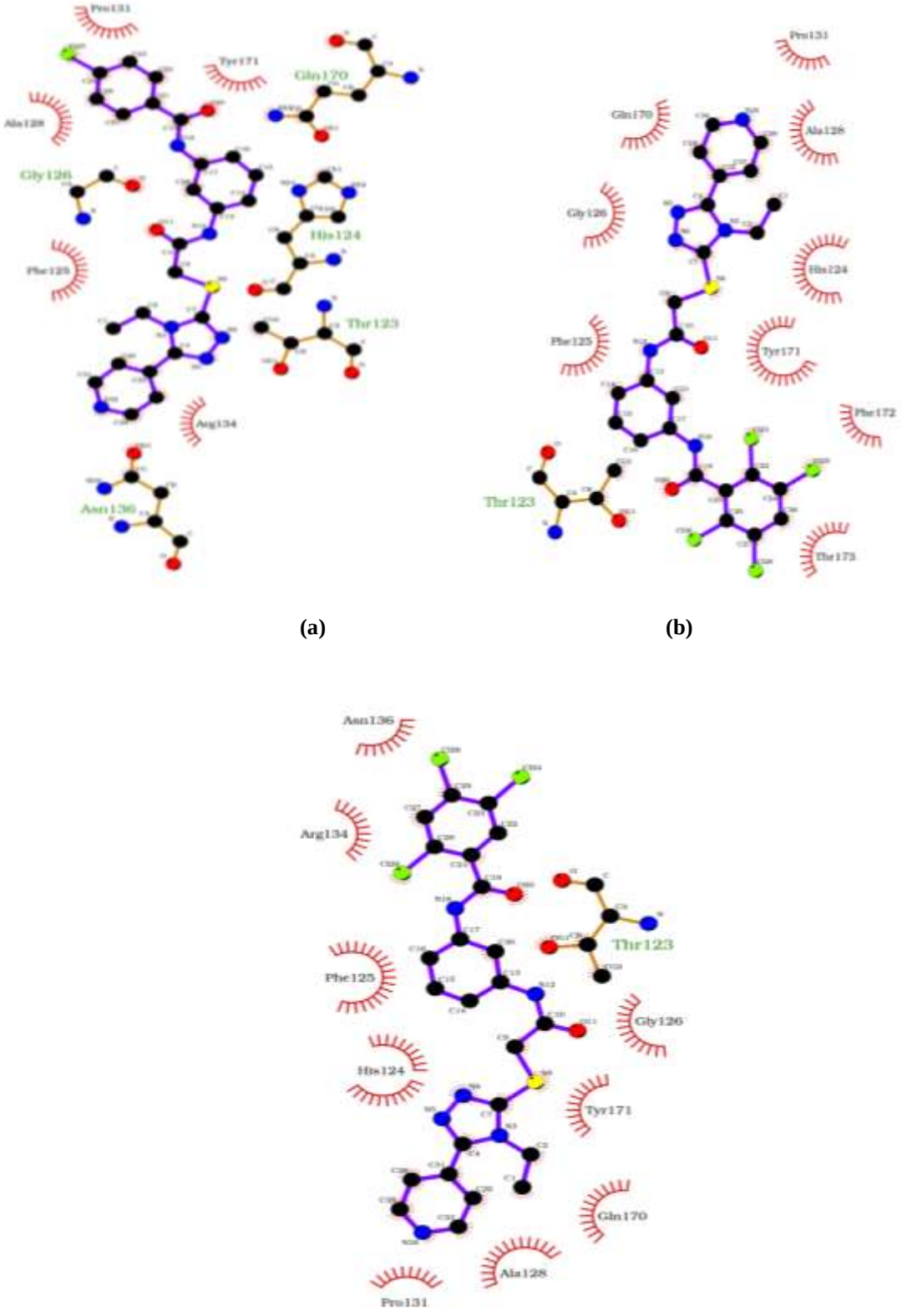

(a) **(b)**

(c)

Figure 5. Hydrophobic interactions of complex protein VP40 with ligand **(a)** M-1, **(b)** M-16 and **(c)** M-11

Based on the docking results and the analysis of hydrogen bond and hydrophobic interactions, all the ligands showed high binding affinities towards VP40, although the binding energies of the modified ligands do not surpass but are comparable to the binding energy of Q-88. It can be deduced that the modification of chlorine atoms on the benzene group does not effectively increase the binding affinity of the complex although it contributes to the hydrophobic interactions.

CONCLUSION

In this study, seventeen ligands were designed to optimise 2-chloro-*N*-[3-[[2-[[4-ethyl-5-(4-pyridyl)-1,2,4-triazol-3-yl]thio]acetyl]amino]phenyl] benzamide (Q-88), which have the potential to inhibit the VP40-RNA binding site. The results showed that all ligands hold high binding affinities with VP40 ranging from -5.5 kcal/mol to -6.9 kcal/mol. Combining previous results with the current work, it was envisaged that the presence of electron donating group such as methoxy substituent may decrease the binding affinity, while the presence of halogens such as fluorine or chlorine may yield better binding affinity. However, it was found that the position and number of chlorine atoms on the benzamide group do not significantly increase the binding affinity of the complex. It is interesting to note that the *para*-position of chlorine atom on ligand M-1 results in the formation of hydrogen bonds with the nearby O and N atoms due to less steric hindrance. This study provides preliminary results on the potential of VP40 inhibitors based on the Q-88 scaffold. Further evaluation on the effect of other substituents such as electron donating groups including other halogens, drug likeness violations and bioavailability, as well as ADME properties of the ligands could help to reduce the cost and time required in computer-aided searches for potential inhibitors to treat the Ebola disease. In addition, molecular dynamics study could also be used to shed more light on the interactions of the molecules.

ACKNOWLEDGMENT

We thank the International Islamic University Malaysia (IIUM) for the facilities provided to conduct the research.

CONFLICT OF INTEREST

The authors declare no conflict of interest.

REFERENCES

1. Gelderblom, H. R. (1996) Structure and Classification of Viruses in *Medical microbiology*, ed. Baron. S. (4th Edition). University of Texas Medical Branch at Galveston: Texas.

2. Kazlauskas, D., Krupovic, M. & Venclovas, C. (2016) The logic of DNA replication in double-stranded DNA viruses: insights from global analysis of viral genomes. *Nucleic Acids Research*, **44(10**), 4551–4552.

3. Raka, L. (2015) Antivirals and antiretrovirals Ebola outbreak in West Africa. *Journal of Antivirals & Antiretrovirals*, **7(1)**, 4172 – 4173.

4. Dhama, K., Karthik, K., Khandia, R., Chakraborty, S., Munjal, A., Latheef, S. K., Kumar, D., Ramakrishnan, M. A., Malik, Y. S., Singh, R., Malik, S., Singh, R. K. & Chaicumpa, W. (2018) Advances in designing and developing vaccines, drugs, and therapies to counter Ebola virus. *Frontiers in Immunology*, **9(8),** 1–15.

5. Hatfill, S. J., Nordin, T. & Shapiro, G. L. (2014) Ebola virus disease. *Journal of American Physicians and Surgeons*, **19(4)**, 101–111.

6. Johnson, R. F., McCarthy, S. E., Godlewski, P. J. & Harty, R. N. (2006) Ebola virus VP35-VP40 interaction is sufficient for packaging 3E-5E minigenome RNA into virus-like particles. *Journal of Virology*, **80(11)**, 5135–5144.

7. Madara, J. J., Han, Z., Ruthel, G., Freedman, B. D. & Harty, R. N. (2015) The multifunctional Ebola virus VP40 matrix protein is a promising therapeutic target. *Future Virology*, **10(5)**, 537–546.

8. Stahelin, R. V. (2014) Could the Ebola virus matrix protein VP40 be a drug target? *Expert Opinion on Therapeutic Targets*, **18(2),** 115–120.

9. Noda, T., Sagara, H., Suzuki, E., Takada, A., Kida, H. & Kawaoka, Y. (2002) Ebola virus VP40 drives the formation of virus-like filamentous particles along with GP. *Journal of Virology*, **76(10)**, 4855–4865.

10. Arslan, A. & Noort, V. (2017) Evolutionary conservation of Ebola virus proteins predicts important functions at residue level. *Bioinformatics*, **33(2)**, 151–154.

11. Palamthodi, S., Patil, D., Sankpal, A., Zarekar, S. & Patil, Y. (2012) Identification of drug lead molecules against Ebola virus: an in silico approach. *Journal of Computational Methods in Molecular Design*, **2(2)**, 76–84.

12. El-Din, H. M. A., Loutfy, S. A., Fathy, N., Elberry, M. H., Mayla, A. M., Kassem, S. & Naqvi, A. (2016) Molecular docking based screening of compounds against VP40 from Ebola virus. *Bioinformation*, **12(3)**, 192–196.

13. Macalino, S. J., Gosu, V., Hong, S. & Choi, S. (2015) Role of computer-aided drug design in modern drug discovery. *Archives of Pharmacal Research*, **38(9)**, 1686–1701.

14. Mohamad Yussoff, M. A., Abdul Hamid, A. A., Abd Hamid, S. & Abd Halim, K. B. (2020) A quest on finding new potential Ebola VP40 inhibitors: molecular docking and molecular dynamics simulation studies (pp. 1 – 25), *Sains Malaysiana*, **49(3)**, 537–544.

15. Abazari, D., Moghtadaei, M., Behvarmanesh, A., Ghannadi, B., Behruznia, M. & Rigi, G. (2015) Molecular docking based screening of predicted potential inhibitors for VP40 from Ebola virus. *Bioinformation*, **11(5)**, 243–247.

16. Wallace, A. C., Laskowski, R. A., Thornton, J. M. (1995) LIGPLOT: a program to generate schematic diagrams of protein-ligand interactions clean up structure. Protein Eng., **8(2)**, 127–134.

17. Claußen, H., Buning, C., Rarey, M. & Lengauer, T. (2001) FLEXE: Efficient molecular docking considering protein structure variations. *Journal of Molecular Biology*, **308(2)**, 377–335.

18. Vargas, J. A. R., Lopez, A. G., Pinol, M. C. & Froeyen, M. (2018) Molecular docking study on the interaction between 2-substituted-4,5-difuryl imidazoles with different protein target for antileishmanial activity. *Journal of Applied Pharmaceutical Science*, **8(3)**, 14–22.

19. Tamilvanan, T. & Hopper, W. (2013) High-throughput virtual screening and docking studies of matrix protein VP40 of Ebola virus. *Bioinformation*, **9(6)**, 286–292.

20. Trott, O. & Olson, A. J. (2011) AutoDock Vina: Improving the speed and accuracy of docking with a new scoring function, efficient optimization and multithreading. *Journal of Computational Chemistry*, **31(2)**, 455–461.

21. Hoenen, T., Volchkov, V., Kolesnikova, L., Mittler, E., Timmins, J., Ottmann, M., Reynard, O., Becker, S. & Weissenhorn, W. (2005) VP40 octamers are essential for Ebola virus replication. *Journal of Virology*, **79(3)**, 1898–1905.

22. Mirza, M. U. & Ikram, N. (2016) Integrated computational approach for virtual hit identification against Ebola viral proteins. *International Journal of Molecular Sciences*, **17(11)**, 1–23.

23. Varma, A. K., Patil, R., Das, S., Stanley, A., Yadav, L. & Sudhakar, A. (2010) Optimized hydrophobic interactions and hydrogen bonding at the target-ligand interface leads the pathways of drug-designing. *PLoS ONE*, **5(8)**, 1–8.